

Optics Specifications for 7-BM

Eric Dufresne MHATT-CAT, Bldg 432D
Internal Report BM-2003-1-v1

Nov 8, 2003

Abstract

MHATT-CAT intends to complete its 7BM beamline within the next two years to complete a state of the art bending magnet beamline. It will be designed to be simple to operate, yet flexible enough to provide a variety of X-ray beams in the 7BM-B hutch. This document provides the most current design parameters for the 7BM optics. The bending magnet reflective optics will consist of a large vertically reflecting bendable toroidal mirror procured from Oxford, followed by a small flat mirror placed in the 7BM-B hutch to return the beam horizontally. This document describes both mirror designs.

1 Introduction

Within the next year or two, MHATT-CAT will complete its 7BM beamline to make it into a state of the art beamline. The science planned for 7BM will consist mainly of transmission and fluorescence EXAFS experiments from the UofM Chemistry Dept., general crystallography, and time resolved experiments on condensed matter systems or fluids where the reciprocal space resolution does not require the beam from 7ID. A Huber 6-circle diffractometer in 7BM-B will enable diffraction measurements on thin films and surfaces. The monochromator will be completed for ease of energy scanning for EXAFS experiments. Most of the monochromator components have been procured. The internal crystal mounts and translation mechanisms remain to be fabricated or procured, but similar designs are in operation at PNC and BESRC-CAT. Apart from focusing and collimating mirrors, MHATT-CAT's BM components are already installed in 7BM-A (white beam slits, shutter and beam stop). This document describes the proposed final optical design for 7BM and defines the mirror characteristics required to achieve the scientific program cited above.

Table 1 shows the 4 different planned modes of operations for 7BM. We plan to have a monochromatic beam focused down to 25 (V) by 100 (H) μm FWHM using a toroidal mirror. A focussed pink beam will also be available to allow to set different optical schemes housed in the 7BM-B hutch. Wider bandpass beams for example could be available in 7BM-B with the use of a multilayer. Gains of a factor 10-100 over Si resolution are possible with such optics.

Mode	Power density (W/mm ²)	Energy range (keV)	Bandpass (% at 10 keV)	Beam size on sample (mm)
White beam on 7ID	200	5-100	2.5	2.07(H)by 0.65(V)
Focussed mono	0.11	3.7-20	0.014 (or 0.076)	0.15(V) by 0.1(H)
Focussed pink	1.9×10^3	5-20	-	0.15(V) by 0.1(H)
Unfocused mono	11×10^{-6}	3.7-27.5 (11.1-82.5)	0.076	187(H)by 4(V)
Unfocused white	0.64	5-100	-	187(H)by 4(V)

Table 1: MHATT-CAT 7BM-B Beam properties for the four proposed modes of operations, 36 m from the source with a two mirror design. In unfocused mono mode, a Si (333) could diffract up to 80 keV X-rays. The beam size in 7BM-B would depend on the width of the first crystal. In focussed mono mode, the bandwidth for a one mirror design is shown in parenthesis. The X-ray beam divergence incident on the sample would be around 3.6 mrad and 0.6 mrad in the horizontal and vertical directions respectively for the focussed beams. See Table 6 for details.

A white beam will be available as well in 7BM-B for high energy diffraction experiments. With the mirrors translated down, the unfocused monochromatic mode will allow to provide Si (333) resolution up to about 80 keV.

The 7BM will be a very important addition to the beamtime available at sector 7. Unlike several sectors, the 7ID beamline does not use time sharing, multiple undulators, or beam sharing by splitting the beam with mirrors. Apart from time sharing the beam between hutches 7ID-C and D, only one experiment can be done on 7ID at one time. Thus making the 7BM a versatile and state of the art beamline will help the sector to provide more beam time for less brilliance-limited experiment. This will free the ID line for experiments requiring higher resolution or transverse coherence.

The beamline components already procured are a white beam slits and lead collimator which can theoretically accept up to 5.3 mrad of the bending magnet's horizontal fan (in practice, a focusing mirror could only use about one mrad). A double crystal fixed offset (35 mm) Si (111) monochromator will provide beams from 3.7 to 27.6 keV. A P6 shutter is also installed and allows to select either white or monochromatic beam operation. The focusing optics is discussed next.

1.1 A two mirror design

Our final design rely on one large Oxford-Danfisik U-Bender toroidal mirror reflecting upwards installed in the 7BM-A followed by a small flat mirror reflecting downward housed near the Huber 6-circle in 7BM-B. Fig. 1 shows a cartoon of the beamline layout. The beamline would consist of a white beam Be commissioning window, followed by a white beam slit, a monochromator, a P6 shutter, a toroidal mirror, then the small flat mirror. The two mirrors deflect the beam vertically with a grazing angle of incidence of 3.2 mrad. Both mirror substrates are made from Si, with a Rh coating which sets the critical energy to 20 keV. Both mirror will be water-cooled, but the second mirror may simply require indi-

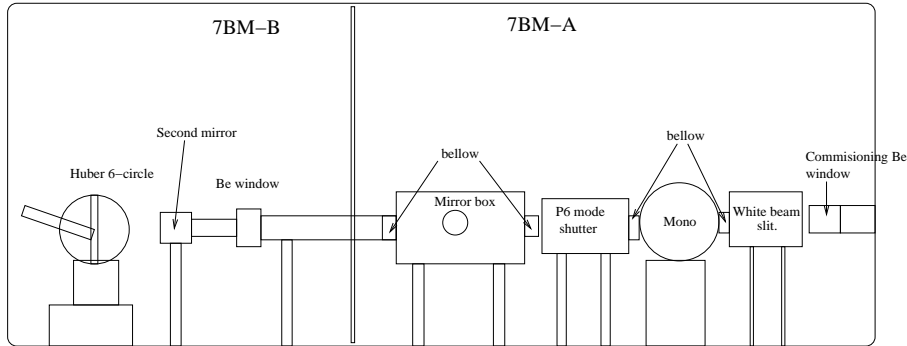


Figure 1: The simplified beamline layout for 7BM.

Technical characteristic	
Monochromatic energy resolution at 10 keV (eV)	6.5
Demagnification H(V)	3.55 (3.55)
Expected focal spot H (V) (μm)	100 (150)
depth of focus (cm)	10
divergence on sample H(V) (mrad)	3.6 (0.53)
Horizontal fan accepted (mrad)	1.0

Table 2: A summary of the focussed monochromatic beam, based on Table 6.

rect water cooling when pink beam operation is selected. MHATT-CAT has already started procurement of the first focusing mirror using funds raised from the Michigan Life Science Initiative. The delivery is expected in August 2004, and the mirror purchase will be well over 300 k\$. This design will have an energy resolution a factor 4-6 worse than if one were to use a collimating optics in front of the monochromator (see Table 2 and 4), but if one needs Si (111) energy resolution, the white beam slit vertical opening can be reduced to improve the energy resolution of the monochromator.

After the focusing mirror, the beam would climb up with a 6.4 mrad angle, and if one were to take the mirror out, the 7BM-B Huber table would have to move down 52 mm. Note that our Huber 6-circle motorized table does not tilt. Since our diffractometer program SPEC requires the beam to be horizontal in its alignment procedure, the second mirror placed upstream of the diffractometer returns the beam to an horizontal propagation direction. The second mirror would be a short flat mirror (say 30 cm long) next to the sample. It could have two separate coatings, Rh, Si, Pt to filter the X-ray energy from the monochromator. The short flat needs to be procured likely from WavePrecision, and its chamber and motorized stages needs to be designed as well. This should be a relatively inexpensive and straightforward task. Table 2 summarizes the optical design. The optics would essentially focus the beam down to a spot with a FWHM of about 0.15 mm (V) and 0.1 mm (H) (see Fig. 9-11).

This document is intended to give MHATT-CAT users and members a chance to review the optical design of 7BM-A for their projected experiments. Section 2 introduces some of

the background information for the optical design. Section 3 describes the final design.

2 Essential source, slits, and monochromator data, mirror optics

2.1 Known source parameters for an APS BM

The maximum horizontal emittance of the APS is currently approximately $\epsilon_x = 7.0$ nm-rad, and the vertical coupling is about 1 %. The low β_y lattice has now parameters of $\beta_x = 1.64$ m and $\beta_y = 15.9$ m (see Table 3). This lattice has been in force for at least two years now. As shown in Table 3, the source size is $\sigma_x = 145\mu\text{m}$, $\sigma_y = 36\mu\text{m}$, the maximum horizontal fan is $\sigma_{x'} = 6$ mrad and $\sigma_{y'} = 47\mu\text{rad}$ (at the Critical Energy).

For design purposes, we should remind ourselves that for a Gaussian source with rms size σ , the total flux transmitted through an aperture Δ is

$$\text{erf}\left(\frac{\Delta}{2\sqrt{2}\sigma}\right). \quad (1)$$

Computed values for several values of Δ/σ are shown in the Appendix in Table 9. For example, if $\Delta = 4\sigma$, then 95.5 % of the flux is transmitted. Also, note that a Gaussian has a FWHM equal to 2.35σ .

The APS runs currently at 100 mA, but there are possible plans for upgrades to 300 mA, thus detailed thermal calculations should be done for the first mirror. For the time being, I will use the present ring current value of 100 mA to do a preliminary design. In the table above, two sets of beam sizes and emittance are shown. In low emittance mode, the source sizes would be smaller than those used below for calculations, but it would not change the divergences. Thus final focal spots will be overestimates at this point.

Note that the total power is 87 W/mrad of horizontal fan accepted. The on-axis power density is 0.78 kW/mrad², a factor 214 lower than 7ID at closed gap. Our toroidal optics will focus reasonably well a 1 mrad fan. A significant portion of this power would be reflected, some would be absorbed. If the source were to be upgraded to 300 mA, then we would find the total incident power at 261 W, but the absorbed power would be well below the 250 W maximum power of the mirror.

The ring critical energy is defined as the energy where half of the radiated power is below this energy. The critical energy can be calculated from

$$E_c(\text{keV}) = 0.665E^2(\text{GeV})/B(\text{T}), \quad (2)$$

and thus only depends on the ring energy E and the bending magnetic field B . At the APS, $B = 0.6$ T, $E = 7.0$ GeV, thus the critical energy is $E_c = 19.51$ keV. If a grazing incidence mirror critical energy was set to the ring critical energy, than on order of half of the source power would be absorbed in the mirror, thus on order 44 W per mrad for 100 mA operation.

To a good approximation, the vertical source divergence can be modeled by a Gaussian $\exp(-0.5\Psi^2/\sigma_\Psi^2)$, where Ψ is the vertical angle of observation from the optical axis, and

Ring Energy	7 GeV
Ring Current	100 mA (upgrades to 300 mA?)
Single bunch current	5 mA
Bunch length	73 psec
Revolution time	3.68 μ sec
RF frequency	351.93 MHz
Circumference	1104 m
Bend Radius	39 m
Bend field	0.6 T
critical energy	19.51 keV
Energy range	1-100 keV
On-axis power density	0.78 kW/mrad ²
On-axis power	87 W/mrad
α_x	0.46
α_y	0.57
β_x	1.64 m
β_y	15.9 m
η_x	0.093 m
$\eta_{x'}$	-0.068 m
ϵ_x hor. emittance	7 (3.07) nm-rad
ϵ_y vert. emittance	0.066 (0.0367) nm-rad
vertical coupling	0.886 (1.2) %
σ_x hor. source size	145 μ m
σ_y vert. source size	36 μ m
$\sigma_{x'}$ hor. divergence	6 mrad
$\sigma_{y'}$ vert. divergence	47 μ rad (19.51 keV)

Table 3: description of the APS Bending Magnet Source monochromator. (From the APS web site) The number in parenthesis for the emittance are for the low-emittance mode which is the current mode for 75% of the time.

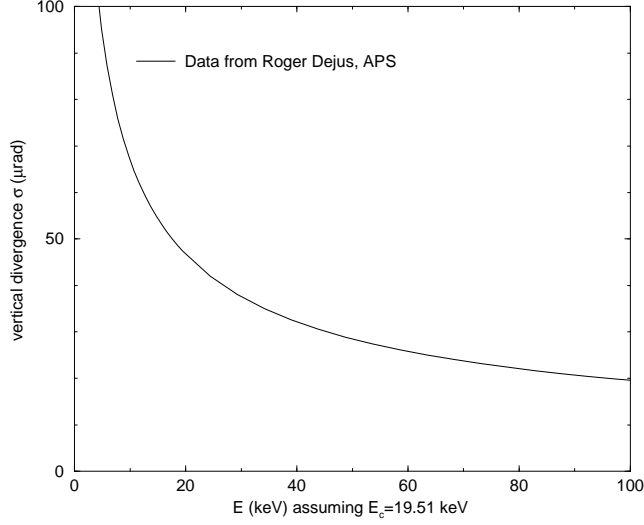


Figure 2: The APS BM vertical divergence. This function affects the monochromator resolution and the fraction of the flux accepted by mirrors.

Energy (keV)	σ_Ψ , rms vertical divergence (μrad)	Mirror $\Delta\Psi$ (in units of source σ_Ψ)	Si (111) θ_B (degrees)	Darwin width (FWHM) (μrad)	$\Delta E/E \times 10^{-4}$
7.0	78	1.64	16.41	42.1	4.6
8.0	73	1.75	14.31	36.4	5.2
9.0	70.6	1.81	12.69	32.1	5.9
10.0	66.6	1.92	11.40	28.8	6.5
11.0	63.7	2.01	10.35	25.9	7.2
12.0	60.5	2.12	9.48	23.8	7.8
14.0	56.3	2.27	8.12	20.1	9.1
16.0	52.3	2.45	7.10	17.5	10.4
18.0	49.2	2.61	6.31	15.5	11.7
19.51	47.3	2.71	5.82	14.3	12.7

Table 4: Some tabulated divergences from Fig. 2. A 1.1 meter long mirror, set to 3.2 mrad, 27.5 m from the source is assumed for the accepted angular flux. In practice, the white beam slit would be closed to limit the vertical beam size to the clear aperture of the mirror. Note that the best figure of the mirror is only specified for the central 0.9 m of the mirror where the figure errors are 0.5 arc sec rms ($\Delta\Psi = 105 \mu\text{rad}$).

σ_Ψ is the energy dependent rms vertical source divergence. Figure 2 shows the vertical beam divergence for an APS bend magnet, data provided by Roger Dejus of the APS. At the critical energy, the rms divergence in the figure agrees well with the tabulated APS divergence presented earlier. The divergence is energy dependent and increases as the energy decreases. Table 4 shows a few tabulated values from Figure 2.

The total focussed beam flux in 7BM-B will be limited by the horizontal and vertical acceptance of the 7BM-A mirror. A vertically deflecting grazing incidence mirror of length L placed a distance d_m from the source and set to an angle θ accepts a vertical angle $\Delta\Psi = L \sin \theta / d_m$. Our mirror is 1.2 m long with a clear optical length of 1.1 m. For a 1.1 m long mirror set to 3.2 mrad and placed 27.5 m from the source, the vertical acceptance is 128 μ rad. For typical crystallography experiments, the mirror would accept about 1.6 to 2.7 source divergence. The reflected flux will thus increase until the critical energy of the mirror. Assuming 100% reflectivity for the mirror, near 7 keV, the mirror would transmit 68 % of the source total flux, while near 20 keV more than 87% would be reflected (see Table 9).

The table also shows the Si (111) Bragg angles using $2d = 6.271 \text{ \AA}$ and its FWHM Darwin width. The source angle σ_Ψ represents about 4-6 Darwin width for typical crystallography experiments in the range of 7-12 keV.

Note that if one were to accept a white beam with vertical divergence $\Delta\Psi$ on a monochromator, then one would expect the energy resolution to be blurred according to

$$\frac{\Delta E}{E} = \frac{\sqrt{\Delta\theta_p^2 + \Delta\Psi^2}}{\tan \theta_B}, \quad (3)$$

where $\Delta\theta_p$ is the FWHM of the monochromator Darwin width and θ_B its Bragg angle[1]. This formula is also shown in Table 4. For Si (111) resolution on 7ID at 10 keV, one typically finds $\Delta E/E = 1.4 \times 10^{-4}$, thus without collimation in front of the monochromator, the energy resolution would be worse by a factor from 3-9 when compared to the ID line. With angular collimation by either slitting down to reduce $\Delta\Psi$, or by using refractive or reflective collimators, the energy resolution could become nearly identical to 7ID's resolution [1]. Slitting down would clearly limit the flux available. With small reflective losses, a collimating mirror would preserve the resolution of Si (111).

2.2 White Beam Slits

The BM slits maximum opening I believe is 120 mm horizontally and 18 mm vertically. Its design position is roughly 22.5 m from the source, thus one could accept up to 5.33 mrad of the horizontal BM fan with these slits. The slits bolted on the floor is a L3 BM H/V Slit, a nice slit with encoders. It is followed by a 120 mm wide lead collimator.

2.3 Monochromator characteristics

The monochromator is a double crystal Si (111) monochromator. Both crystal are rotated simultaneously by an in-vacuum Huber rotation stage. The first crystal is mounted directly

Table 5: description of the 7BM monochromator motors.

Description	Motor type	range of motion
First crystal Bragg angle	Huber with stepper	-5 to 32.2 degree
Table Horizontal Upstream x1	slide and stepper	50 mm
Table Horizontal Downstream x2	slide and stepper	50 mm
Table height z1	stepper with wedge slide	12.5 mm
Table height z2	stepper with wedge slide	12.5 mm
Table height z3	stepper with wedge slide	12.5 mm
Second crystal chi	picomotor	step (0.3 μ rad)
Second crystal theta	picomotor	step (0.3 μ rad)
Second crystal theta	piezo	0-10 V gives 0-300 μ rad
Energy range		3.7-27.6 keV

on the Huber stage, while the second crystal is allowed to be translated with two slides mounted themselves on the Huber. This design keeps the offset constant at 35 mm [2]. The offset is constant for a range of Bragg angle between 4.1 to 32.2 degrees. With a long second crystal, it is possible to move beyond this range, but the offset is no longer constant with the monochromator energy. Using Bragg's law for Si (111), this corresponds to an energy range from 3.7 to 27.6 keV. I have confirmed this range recently with the 7ID monochromator, reaching 24.5 keV in Feb. 2002. The mechanical range of motion and type of actuator is shown in Table 5. Note that the vertical range of the table is only 12.5 mm.

2.4 P6 monochromatic shutter and white beam stop properties

The P6 on 7BM acts essentially as the P4 on 7ID. It passes a monochromatic beam or a white beam, but only one at a time. In white beam mode, an aperture is set to the nominal white beam height. In monochromatic mode a water cooled white beam stop is dropped into the white beam, and a monochromatic aperture passes the monochromatic beam. An additional shutter can be activated to access 7BM-B while beam is in 7BM-A. This allows for keeping the optics warm at all time. The monochromatic aperture is 120 mm (H) by 10 mm (V) and the maximum monochromatic beam power the shutter can take is 10 W. The white beam aperture is 120 mm (H) by 13.3 mm (V) and its maximum power is 1560 W. The P6 is currently bolted to the floor in 7BM, and kept under vacuum. The P6 must be included in the PSS in the future, and it needs to be relocated. For the two mirror solution, some re-engineering must be done to allow the height of the P6 to be moved if the first mirror is lowered.

2.5 Grazing incidence mirrors

In synchrotron beamline optics, grazing incidence mirrors are often used to collimate the source i.e. reduce the source divergence so that it matches the monochromator input Darwin width[1]. They are also used to collect a large fraction of the flux to focus it into a small

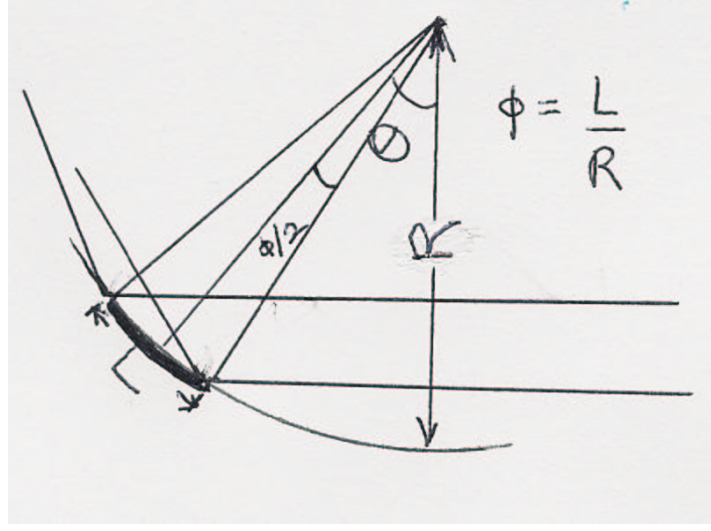


Figure 3: The vertical acceptance of a grazing incidence mirror.

transverse area to match typical sample dimensions. Typically such a scheme uses 1:1, near unity conjugation ratio. On 7ID, we use mirror also with large demagnification factor M (typically around $50 \text{ m} / 0.1 \text{ m} = 500$) to focus the beam on a micron scale for micro-diffraction and fluorescence experiments. The ideal figure to focus a point source to a point at the experiment is an ellipse. To collimate, one wants a parabola such that the point source image is at infinity.

Fig. 3 shows a cartoon of a cylindrically bent grazing incidence mirror of length L with a tangential radius of curvature R , and a grazing angle of incidence θ from the incident X-ray beam. It is easy to show that the vertical acceptance of such a mirror is

$$\Delta y = 2R \sin \theta \sin(\phi/2) \approx L\theta, \quad (4)$$

where $\phi = L/R$. With $R = 3.8 \text{ km}$, $L = 1.1 \text{ m}$, and $\theta = 3.2 \text{ mrad}$, $\Delta y = 3.52 \text{ mm}$. The grazing angle of incidence θ_i will vary over the length of the mirror so that

$$\theta - \phi/2 + \Delta\Psi/2 < \theta_i < \theta + \phi/2 - \Delta\Psi/2. \quad (5)$$

For $R = 3.8 \text{ km}$, $L = 1.1 \text{ m}$, $\Delta\Psi = 0.128 \text{ mrad}$, θ_i would vary by $\pm 81 \mu\text{rad}$. For a Rh coated mirror where $\theta = 3.2 \text{ mrad}$, this implies that the critical energy over the length of the mirror varies by about 5%. Thus if the mirror center critical energy is set to 20 keV , $E_c = 20.0 \pm 0.5 \text{ keV}$ and varies over the length of the mirror.

At grazing incidence, we define two focal lengths for a spherical mirror of radius of curvature R [3]. The meridional or tangential focal length f_m is

$$f_m = R \sin \theta/2, \quad (6)$$

where θ is the grazing angle of incidence with respect to the surface of the mirror. This focal length focuses the beam along the propagation direction. One also defines a sagittal focal

length f_s such that

$$f_s = R/(2 \sin \theta). \quad (7)$$

This is the focal length for the direction transverse to the tangential plane of incidence. The ratio of $f_m/f_s = \sin^2 \theta$, thus the meridional focal length is always foreshortened, except for the case of normal incidence[3]. This causes severe astigmatism for spherical mirrors. Typically on an X-ray beamline, one can focus in two dimensions using a toroidal mirror having different tangential and sagittal radii, or focus horizontally and vertically with two independent mirrors. This latter scheme is called a KirkPatrick-Baez scheme (KB). For calculating the radius of curvature of the 7BM mirrors, we also need to use the thin-lens formula

$$1/f = 1/i + 1/o, \quad (8)$$

where o and i are the source-mirror and mirror-image distances. The demagnification ratio

$$M = d_i/d_o = i/o, \quad (9)$$

where d_i and d_o are respectively the image and source sizes. To make a cylindrical or parabolic figure, one can either polish a blank to a fixed radius of curvature, or bend a flat mirror with appropriate moments. In any fabrication processes, errors will occur between the ideal figure and the actual figure. They are measured optically with the height of the top surface. On short length scales (< 0.1 mm?) these height variations are called roughness, and are typically measured in Å. Over length scales comparable to the mirror length, these height difference are called figure errors and are typically reported as a slope error in μ radians.

The critical angle θ_c of a material is a function of its index of refraction decrement δ , with

$$\theta_c = \sqrt{2\delta}. \quad (10)$$

Fig. 4 shows the critical angle versus energy for Pt and Rh coatings. If one were to set the critical energy at 20 keV, Rh would have a critical angle of 3.2 mrad, Pt, 4.15 mrad.

Fig. 5 shows the square of the reflectivity versus energy for Rh and Pt set up with a critical energy of 20 keV with critical angles stated above. A 3 Å roughness was assumed in the calculation. Above 11.5 keV, Pt performs worse than Rh due to several absorption edges above this energy. The reflectivity square provided by these parameter is a few percent near 20 keV, and thus would not provide very significant third harmonic rejection when the monochromator is set below 7 keV or so. Additional harmonic rejection could be added in 7BM-B near the sample for specific experiments.

3 Detailed final design.

The focusing mirror introduced earlier is a toroidal mirror. Our design recommends to set both mirror critical energy to 20 keV. We propose using Rh for its high reflectivity and featureless curve. Absorption edges are either well below 5 keV or above 20 keV. The grazing angle of incidence θ is thus 3.2 mrad. The P6 operating in white or monochromatic mode

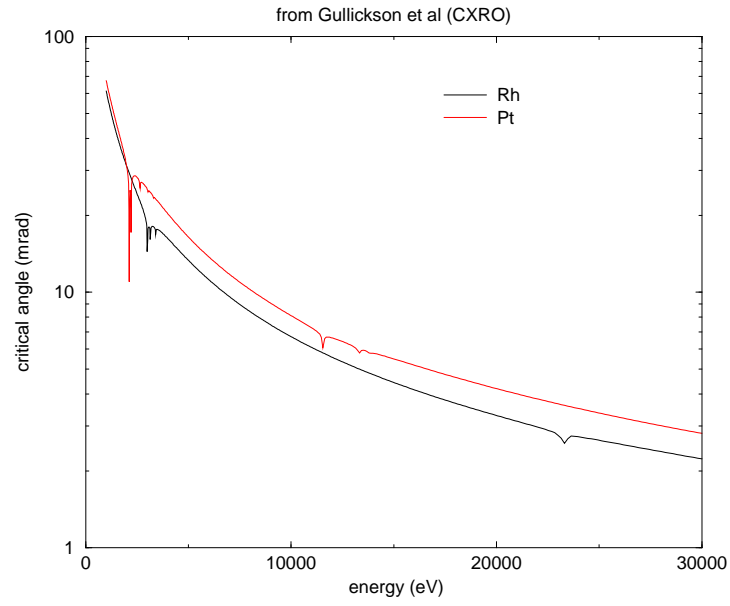


Figure 4: The critical angle for Rh and Pt coating.

Figure 5: The square of the reflectivity for Rh and Pt coatings for a two bounce mirror system.

would be reinstalled and configured as any P6 is around the ring. By moving the mirror vertically in the monochromatic beam, we would have a doubly focussed monochromatic beam in 7BM-B. By moving the water-cooled mirror into the white beam, we could send a pink beam in 7BM-B. By moving the mirror out of the white beam, we could have a full white beam in 7BM-B. No major realignment of the monochromator would be required when going to white beam. The advantage of this optical design is that it reduces the alignment efforts during beamline operation and yet allows a very versatile beamline.

This option could have improved performance through the use of refractive collimators. Through the use of a Li or Be collimator placed upstream of the monochromator tank, one could improve the resolution with improvements over simply slitting down. Figure 6 shows that a Li collimator at 9 keV would have a FWHM of 2.7 mm which is 77% of the 3.5 mm mirror acceptance. Slitting down to keep a Si (111) Darwin width would limit the beam to about $27.7 \text{ m} \times 33 \text{ } \mu\text{rad} = 0.9 \text{ mm}$. The Li or Be collimator would have to be water cooled, and thermal calculations would have to be done to ensure Li can be safely used in 7BM. Fortunately, due to several Be windows upstream of the lens, most of the low energy flux would be absorbed already. Be collimators are already commercially available and Li would be interesting to pursue.

To derive the bend radius for this mirror, the sagittal and meridional focal length are identical, thus $fs = fm = f$. From Eq. 6-7, the meridional radius is

$$Rm_{m1} = 2f/\theta = 2(1/(d_e - d_{m1}) + 1/d_{m1})^{-1}/\theta, \quad (11)$$

where d_e is the source-experiment distance, and d_{m1} is the source-mirror distance. The sagittal radius is

$$Rs_{m1} = 2f\theta = 2(1/(d_e - d_{m1}) + 1/d_{m1})^{-1}\theta. \quad (12)$$

Table 6 shows the final parameters for a one mirror system. Note that the minimum meridional radius for this bender is 3.0 km. From this radius, one can deduce a minimum working distance for the mirror. Table 3 shows the effect of changing the meridional radius and the incidence angle to focus the X-rays at various distance from the source R_e . The closest distance should be 34.4 m, 1.1 m in front of the Huber, while the largest distance of 38 m is in front of the back wall Pb beam stop. To push the critical energy beyond 20 keV, one would have to set up an experiment at the end of the hutch. Note also that we can unbend the meridional radius to mostly focus only in the horizontal direction. This may have the advantage of reducing the vertical divergence on a fairly large sample.

3.1 Spectral calculations with XOP

A useful tool for calculations of spectral properties of synchrotron radiation is called XOP and can be downloaded from the ESRF web site. The software allows for ID and BM simulations. Table 8 shows a brief summary of the simulations. Here two Rh mirrors reflect the beam by 3.2 mrad. We assume a 3 Å rms roughness. We assume that the commissioning window that is currently installed is made of two 254 μm thick Be foils. The XOP simulation

θ	3.2 mrad
d_{mono}	24.7 m
d_{P6}	after mono
d_{m1}	27.7 m
d_e	35.5 m
f	6.09 m
Demagnification H(V)	3.55(3.55)
ideal focal spot H (V)	96 μm (24 μm)
Expected focal spot H (V)	100 μm (150 μm)
depth of field	10 cm
divergence on sample H(V)	3.6 mrad (0.53 mrad)
Rm_{m1}	3.804 km
Rs_{m1}	39 mm
Horizontal fan accepted	approx. 1 mrad

Table 6: Calculated optical radii for a one toroidal mirror design. The ideal focal spot is the demagnified image of the source. The expected FWHM focal spots includes optical aberrations observed in the Shadow simulations (See section 3.2).

distance from source	θ_c	E_c
R_e (m)	(mrad)	(keV)
34.4	3.60	18.3
35.5	3.20	20.0
36.5	2.92	22.2
37.5	2.69	24.3
38.0	2.60	25.4

Table 7: Effect of tilting the mirror and adjusting the meridional radius to focus inside the hutch. The critical energy changes accordingly.

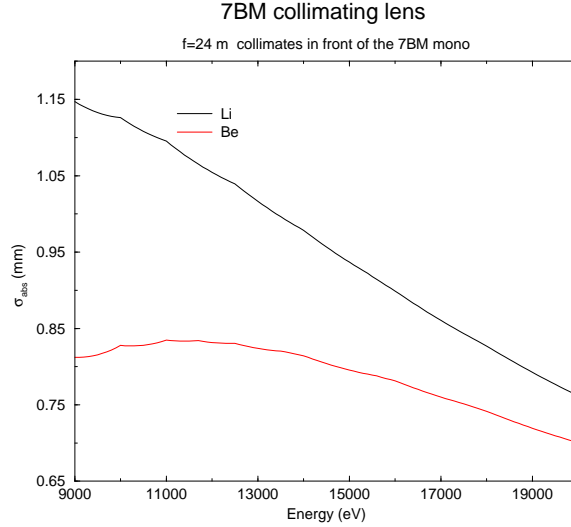


Figure 6: The absorption aperture of a Li (black) and Be (red) collimator for 7BM. For Li, one could collimate a FWHM beam of 2.7mm out of the 4.16 mm wide beam accepted by the mirror.

results for the critical energy and linear power density are consistent with Table 3. The Be window absorbs about 10.4 W; mirror 1, 40.9 W; and mirror 2, 3.9 W.

In the event that the APS was ever run at 300 mA, the absorbed power on mirror one might climb up to 123 W, which is well below the cooling power that Oxford specifies (250 W). In the event of a future current hike, mirror 2 would absorb about 12 W, so we should be able to set the cooling specs on mirror 2 to be at most 15 W. It is nice to keep our optics at a fixed temperature so that heating effects are reduced as much as possible. Remember also that cooling on mirror two is only required if we have pink beam. With a monochromatic beam, mirror 2 would not be heated at all.

Note that the **pink** beam would melt most samples! If the whole pink beam was focussed into a spot of $(150 \times 100) \mu\text{m}^2$, then the power density would be about about $1900 \text{ W}/\text{mm}^2$, or a factor 10 larger than on the unfocused ID line ($200 \text{ W}/\text{mm}^2$). One could do thermal annealing with the pink beam on small spot sizes. This beam would be for special monochromators, such as Si (220) or multilayers placed after the mirror, and well before the experiment in 7BM-B. Most optical elements would not work well at the focal spot.

Fig. 7 shows the spectral monochromatic flux at 7 BM, ignoring an exit Be window in 7BM-B. The low energy flux from the source is heavily absorbed by the commissioning window. The photon energies above the mirror critical energy are also heavily absorbed in mirror 1. The peak flux would be around 10 keV with a total flux of $2.2 \times 10^{12} \text{ ph/s}/100\text{mA}$. If one includes the vertical divergence acceptance of 60 %, then one may hope to reach a total flux near $1.3 \times 10^{12} \text{ ph/s}/100\text{mA}$. A flux on the order of a few $\times 10^{12} \text{ ph/s}$ is what is used in a typical experiment on 7ID. With focusing optics of course, this flux could be available on a small spot size, but the focusing optics becomes quite inefficient as the horizontal fan is increased above 1 mrad. Some optical simulations of 7BM are presented in the next section

bend radius	39m
calculated bend field	0.599 T
hor. divergence	1 mrad
Critical energy	19.51 keV
total power	86.7W
mirror angle	3.2 mrad
mirror roughness	3 Å
Absorbed power in Be Window	10.4 W
Total power after Be Window	76.3 W
Absorbed power in mirror 1	40.9 W
Total power after mirror 1	35.4 W
Absorbed power in mirror 2	3.9 W
Total power after mirror 2	31.5 W

Table 8: Summary of results from a spectral calculation by XOP for one mrad acceptance.

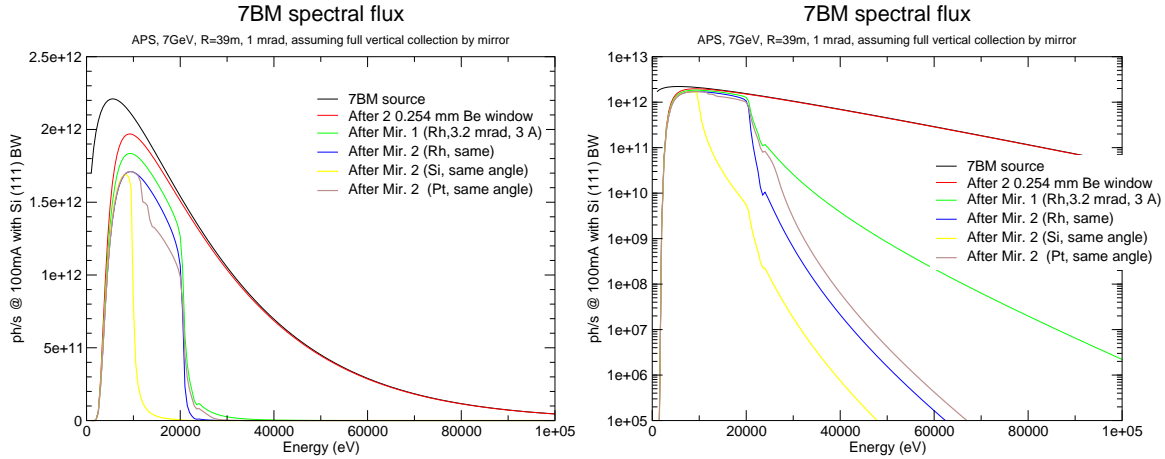


Figure 7: The calculated monochromatic spectral flux.

to show how optical aberrations affect the focal spot. Mirror 2 could be coated with stripes of bare Si, Rh and Pt allowing different cutoffs for low energy experiments. The effect of the three coating is shown in details in the figure.

3.2 Optical ray tracing simulations with Shadow

Detailed ray tracing were completed using the shadow VUI of XOP. A toroidal surface was modeled following the parameters of table 6. A slit was placed in front of the mirror to limit the horizontal acceptance of the mirror.

Fig. 8-11 show the results of four simulations from Shadowvui for a 2.5, 10, 20 and 39 mm horizontal opening. When one uses a narrow slit like in Fig. 8, the focus is about 40 (V) by 100 (H) μm , thus quite comparable to the demagnified image ideally about 25 (V) by

100 (H) μm . Such a small beam on the toroidal mirror could be used to prefocus the beam in front of a KB mirror for microprobe work, thus increasing the aperture significantly from the typical 0.25 by 0.25 mm aperture of our short KB mirror system.

The focal spot becomes wider as the input slit is opened, and for the 39 mm opening, the vertical FWHM of the focal spot is around $150\mu\text{m}$, thus about six times worse than the ideal image. A large vertical tail is present and includes more flux than the integrated intensity around the peak. The results for 20 and 39 mm clearly show the expected inverted U shape from a toroidal mirror. Significant aberrations are present with this optical design. Toroidal optics is best used near unit conjugate ratio, but in our optical design, the demagnification is about 3.5:1.

We will need to use a slit in front of the experiment to isolate the peak from this tail. Although not ideal, this optics will provide a focused beam after slits which will be more or less smooth and on the order of 0.1 mm by 0.1 mm. It will allow a very versatile time-resolved, spectroscopy and scattering program to flourish.

3.3 Possible upgrades, after thoughts.

A natural upgrade would be to install a sagittal bender on the second monochromator crystal. Since most commercial designs operate with a demagnification ratio of 3:1, our beamline layout is ideal for improving the quality of the focal spot. We could get perhaps up to 2 mrad with such an optic. This bender would extend the range of the focussed monochromatic beam to 87 keV since we could focus down the Si (333) diffracted beam (see Table 1). If one were then to add a small focusing mirror (30cm, bendable) after the toroidal mirror, one could use the small mirror with the sagittal bender to provide a smaller focal spot on the Huber than by using the toroidal mirror. This monochromatic beam energy resolution would be close to the Si (111) resolution, but would accept about 20% of the vertical source fan.

4 Appendix

Table 9 shows the computed values Δ/σ in Eq. 1. Designing an optical element that intercepts 87 % of the total flux requires one to make the vertical acceptance $\Delta = 3\sigma$ for example.

References

- [1] J.C. Lang, G. Srajer, J. Wang, P.L. Lee, Rev. Sci. Instrum. **70** 4457 (1999).
- [2] M. Ramanathan et al., Rev. Sci. Instrum. **66**, 2191 (1995).
- [3] X-ray Science and Technology, Edited by A.G. Michette and C.J. Buckley, IOP Publishing, London, Chapter 7, 1993.

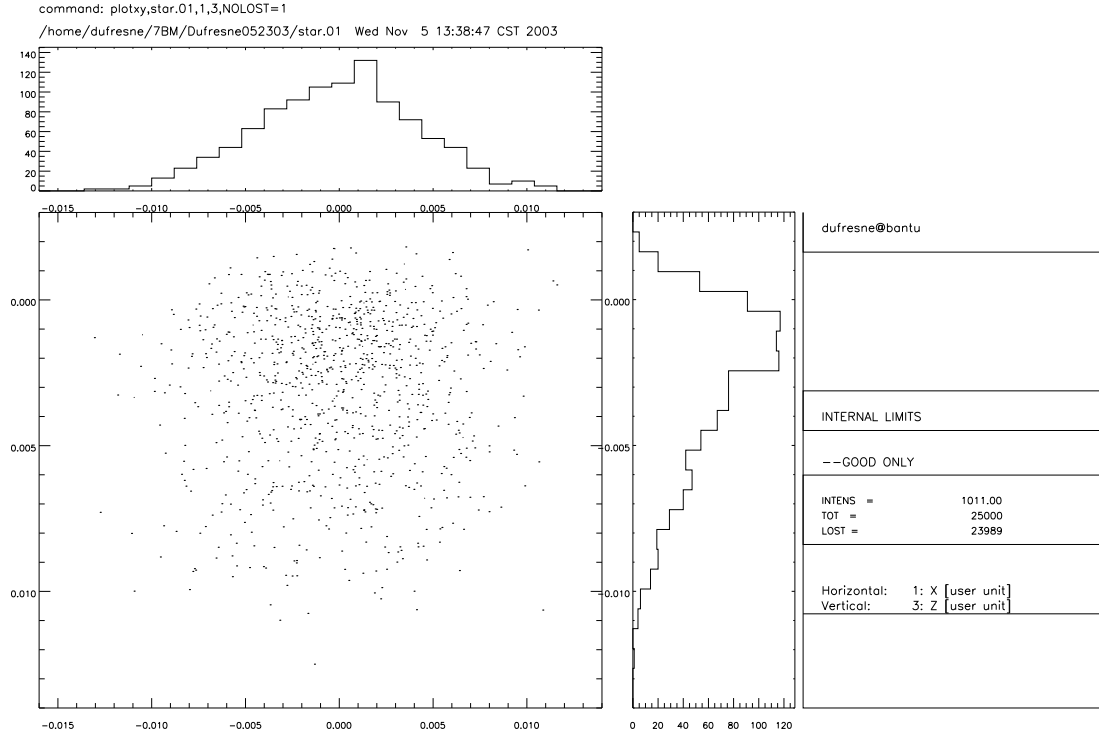


Figure 8: The simulated focal spot from Shadow for a 2.5 mm input beam on the mirror. The spatial units are cm, the vertical histograms are in number of rays, and the fraction of source ray lost is shown. The beam is about 0.05 mm (V) by 0.1 mm. (H)

Δ/σ	Transmitted fractional flux (%)
0.5	19.7
1.0	38.3
1.5	54.7
2.0	68.3
2.35	76.0
2.5	78.9
3.0	86.6
3.5	92.0
4.0	95.5

Table 9: Some tabulated values of Eq. 1.

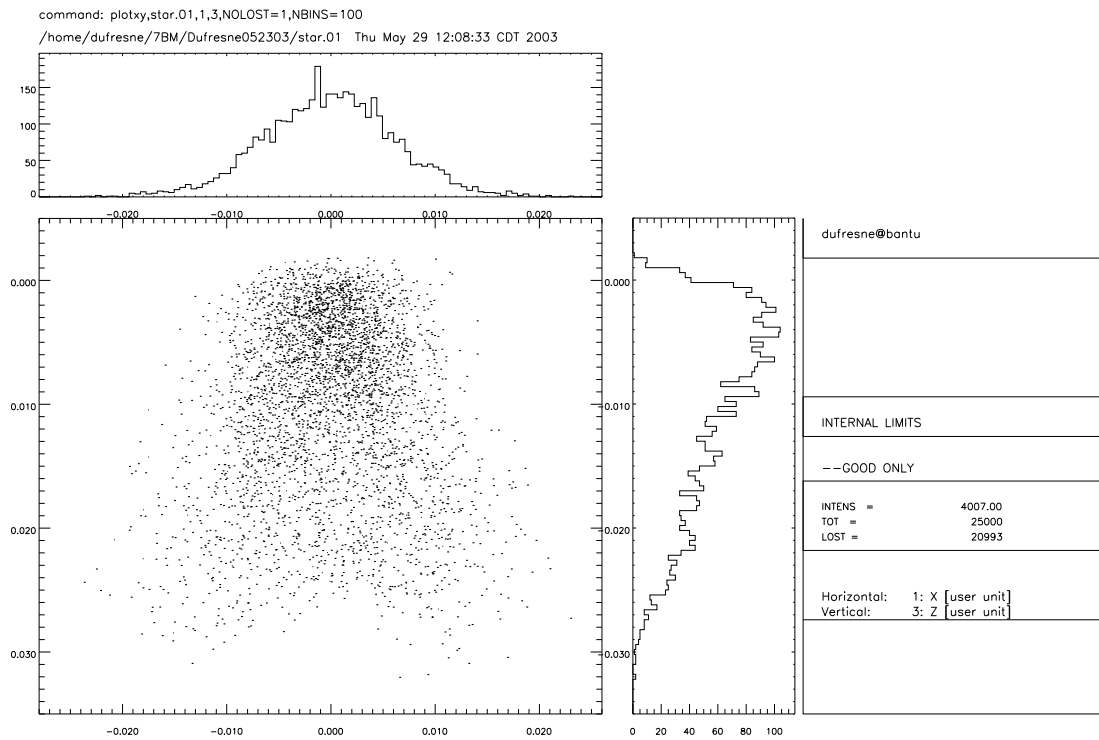


Figure 9: The simulated focal spot from Shadow for a 10 mm input beam on the mirror.

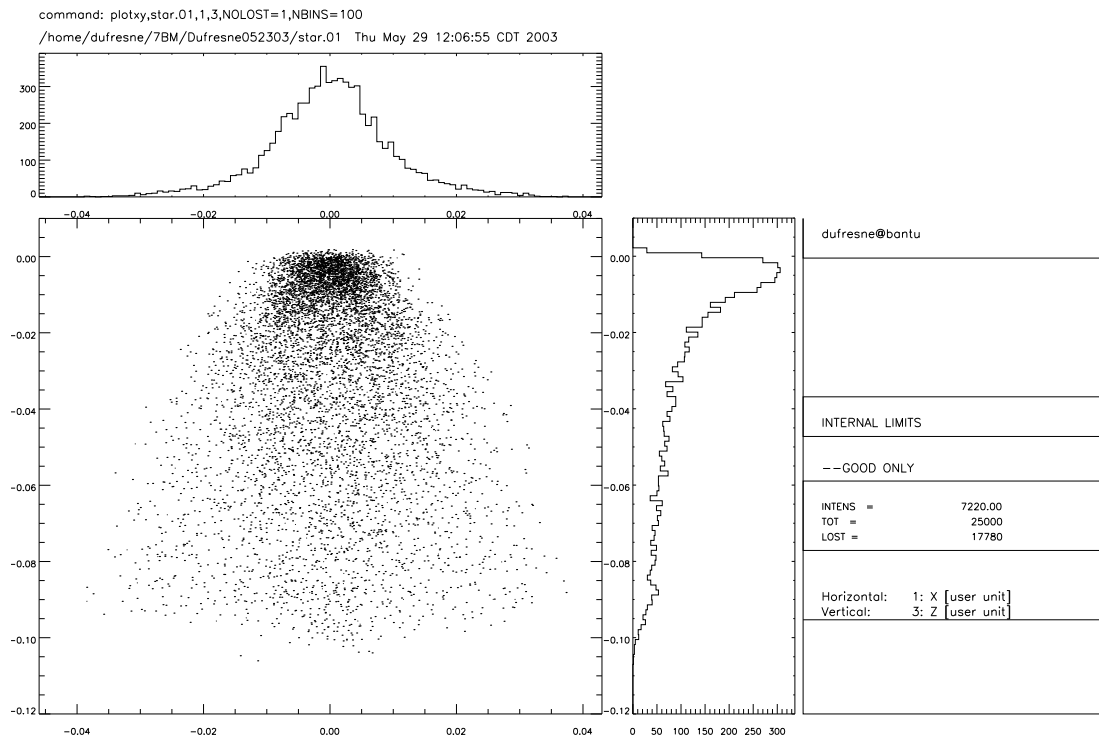


Figure 10: The simulated focal spot from Shadow for a 20 mm input beam on the mirror.

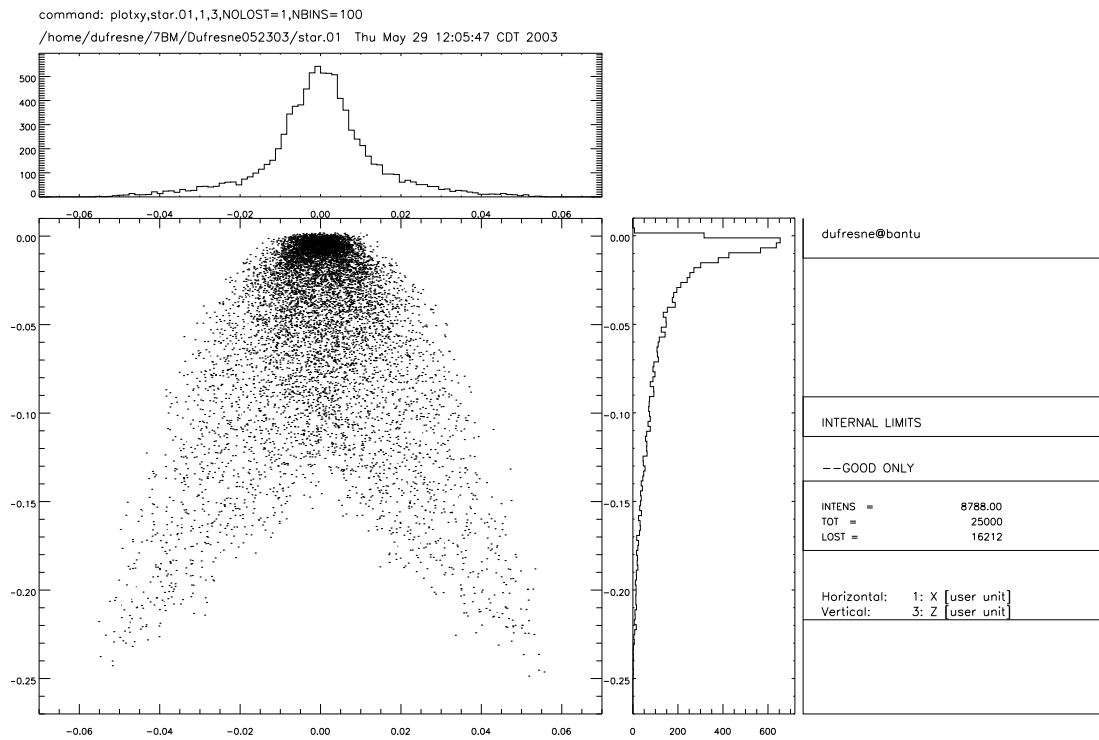


Figure 11: The simulated focal spot from Shadow for a 39mm input beam on the mirror.